

SSSSeg: An Automated Semantic Segmentation Strategy for Hydrogel Scaffolds Based on PBI-μCT



Xiao Fan Ding¹, Xiaoman Duan¹, Naitao Li¹, Daniel Chen^{1,2}, Ning Zhu^{1,3}

¹ Division of Biomedical Engineering, ² Department of Mechanical Engineering, ³ Canadian Light Source Inc.

Contact: xiaofan.ding@usask.ca

INTRODUCTION

In the past ten years, semantic segmentation has been made less laborious with the advent of supervised deep learning techniques. However, many such studies use a data-driven approach that rely heavily on publicly available databases. Such a database does not exist for hydrogel scaffolds. Instead, a physics-driven deep-learning approach may be pursued using synchrotron radiation (SR) propagation-based imaging (PBI) microcomputed tomography (μCT). In PBI-μCT, the phase shift of X-rays between sample and detector manifests as edge enhanced contrast. Quantitatively, where phase shift occurred can be calculated using a phase retrieval (PR) algorithm to get an area contrast image. It is possible to train a convolutional neural network (CNN) to learn the complementary edge enhanced and phase retrieval images to predict a more accurate result than either method alone. This training uses the intrinsic differences in the edge enhanced and phase retrieval images to generate training samples. **This proposed machine learning technique for semi-supervised semantic segmentation (SSSSeg) does not require prior knowledge or manual annotation.**

MATERIALS and METHODS

PBI-μCT scans were performed at the 05ID-2 beamline of Canadian Light Source. Each scan used a 30 keV monochromatic beam. The PBI setup used a SDD of 1.5 m. The detector pixel size was 13 μm, the field-of-view was 26.6 by 6.5 mm, and 3000 projections were collected over 180°. Using these imaging parameters, hydrogel scaffolds made from alginate and gelatin were scanned in vitro.

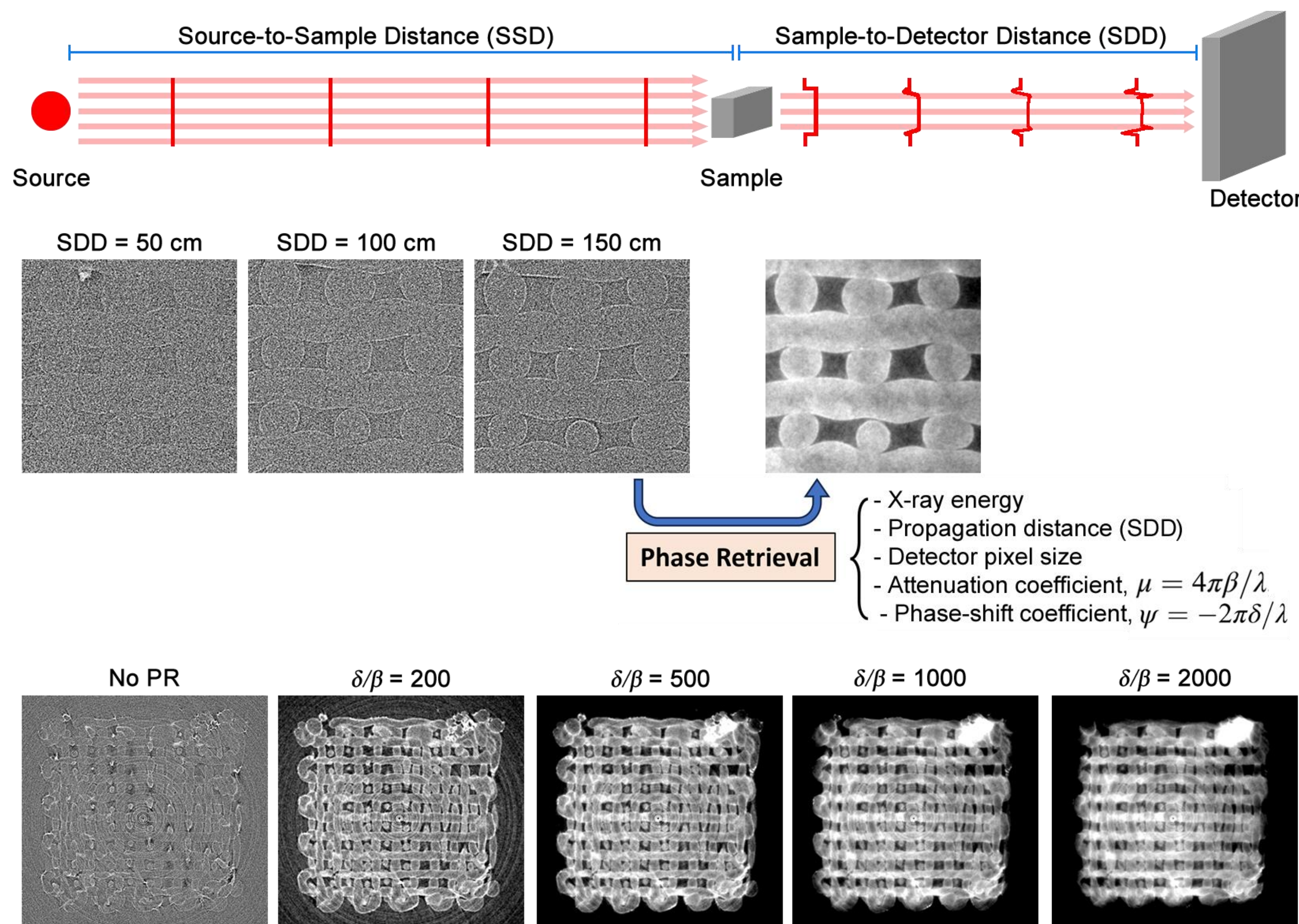


Fig 1: Illustration of how PBI-μCT and the effect of a sample on the X-ray beam. The X-ray passes through a sample and the resulting wave front is distorted by increasing fringes along propagation direction. The fringes manifest as edge enhanced image. Phase retrieval is a technique that quantitatively calculates the thickness of the sample which created such fringes. In hydrogel scaffolds, phase retrieval comes at the cost of well-defined boundaries. The examples shown were imaged with 30 keV parallel-beam X-rays with a detector pixel size of 13 μm. Different SDD show different levels of edge enhanced contrast. Different delta/beta ratios show different degrees of blurring around edges.

Two rounds of CNN training is performed for SSSSeg:

1. Denoising used noise2inverse. A raw dataset was divided into equal splits and reconstructed separately. Both reconstructed stacks should have the same morphological structure, but different noise distributions. **One stack was used as an input and the other was used as the target.**
2. The predicted outcome was a denoised edge enhanced image. The original dataset would then be reconstructed using the TIE-Hom phase retrieval (PR) algorithm. **This time, the denoised edge enhanced stack as the input and the PR stack as the target.**

For both rounds of CNN training, a U-Net architecture, four convolutional layers, 1e-4 learning rate, and SSIM as the loss function were used as shown in Fig 2.

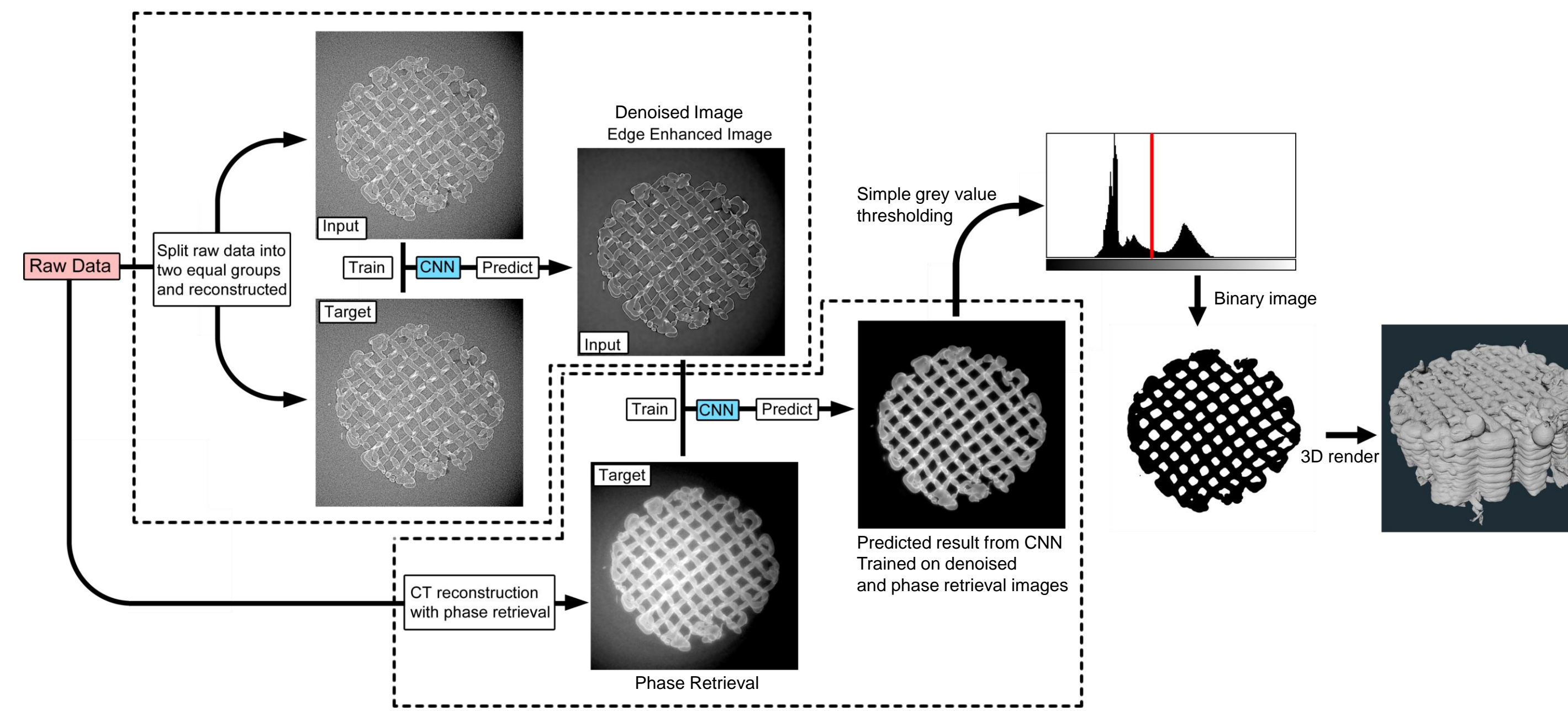


Fig 2: Flowchart for training a CNN with using edge enhanced contrast and phase retrieval images from one dataset. The predicted output yields a greater contrast image than either method alone. CNN training used a U-Net architecture.

RESULTS

The 3D results from the SSSSeg method are compared with other commonly used segmentation methods shown in Fig 2. The most popular methods are interpolation-based methods that require some manual segmentation as input e.g., Biomedisa which uses random walk interpolation, or the simple interpolation method built into Amira-Avizo. SSSSeg eliminates the need for manual segmentation, with the only manual work in determining the best image processing parameters and data preparation, which took approximately 20 min for each sample in this study. The significant difference is that once the image processing parameters are known, they can be incorporated into batch processing for samples of the same or similar material. The semi-manual methods on the other hand, require several hours of pre-segmentation for every sample. In this study, it took 4 hours to manually segment 12 slices before interpolating using Biomedisa. Amira-Avizo used simple interpolation between two slices which is the fastest method but also yield the worst results.

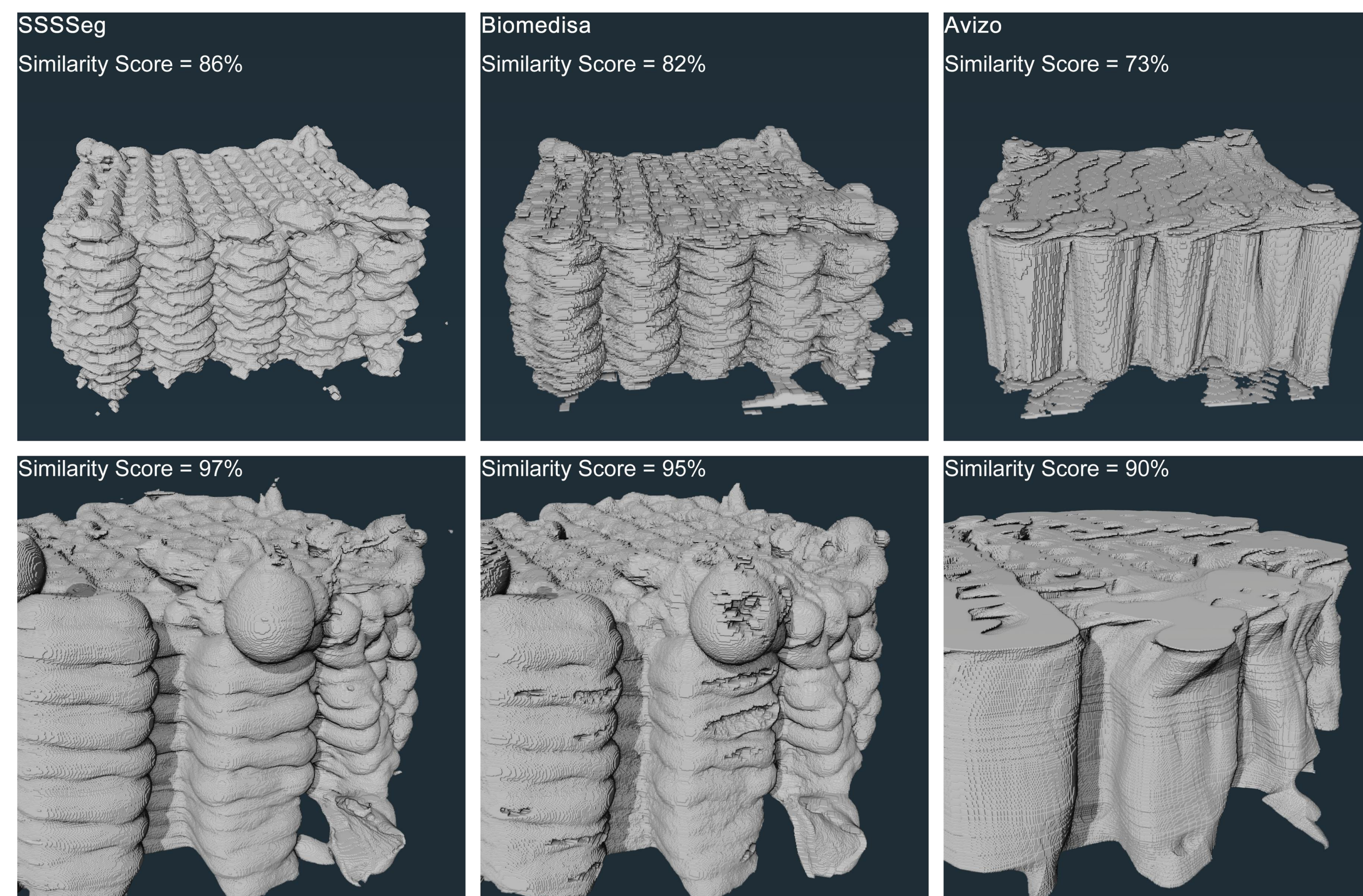


Fig 3: A comparison of SSSSeg, Biomedisa, and Amira against a manual segmentation which is considered ground truth. SSSSeg as a physics-driven semi-supervised method required no manual work compared to Biomedisa and Amira which are both interpolation-based methods which require pre-segmentation. The Dice score was used to as the measurement of similarity to the ground truth.

Shown in Fig 4, there is a noticeable decrease in segmentation quality from SSSSeg with for lower contrast datasets which itself, is result from the physical phenomenon hydrogel scaffolds exhibiting a lower crosslinking degree. At a lower crosslinking degree, the scaffolds were more water-swollen, leading to a lower interaction with X-rays, and thus, the lower signal-to-noise ratio (SNR) and contrast-to-noise ratio (CNR) measurements.

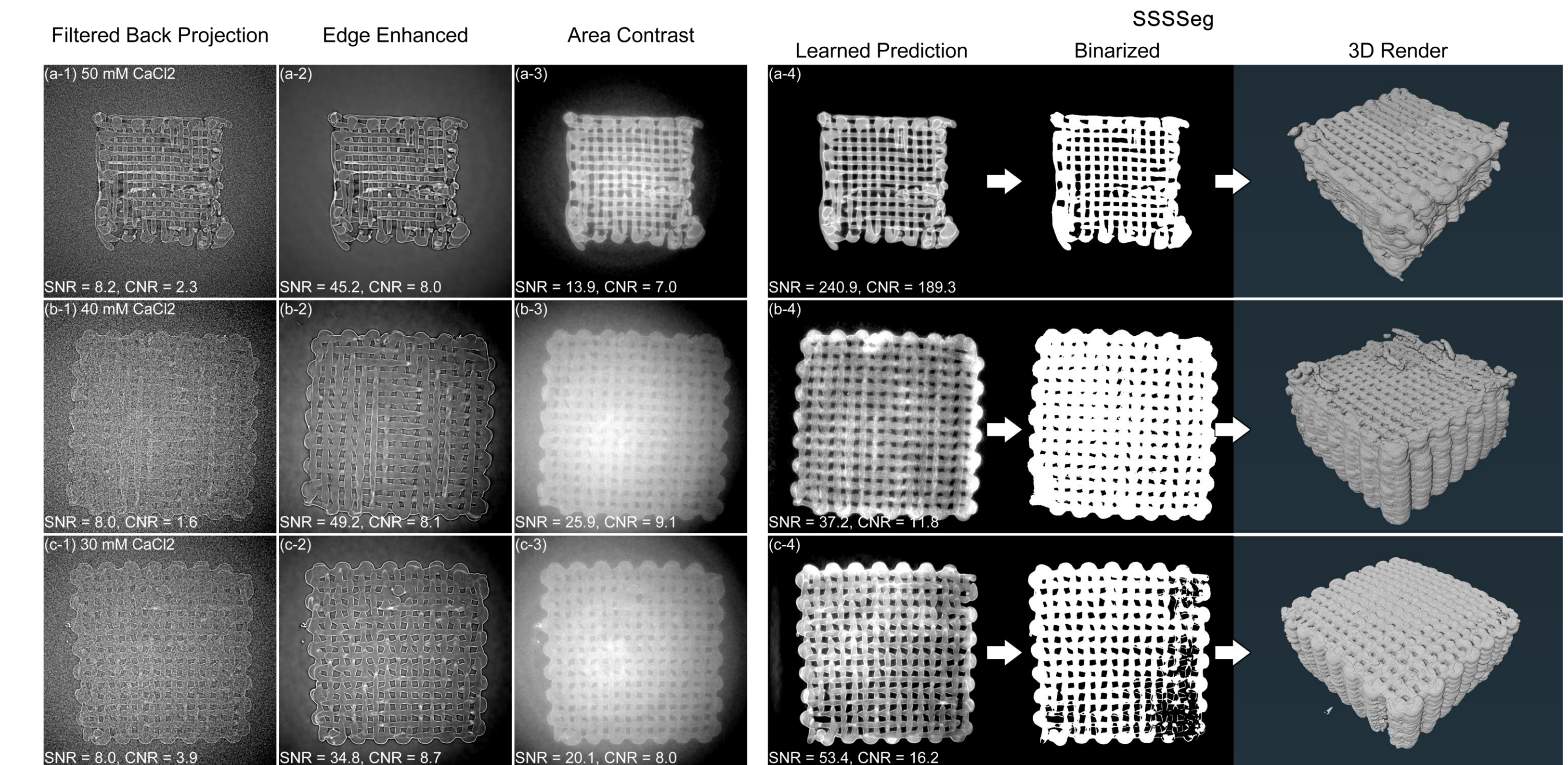


Fig 4: Demonstration of SSSSeg on hydrogel scaffolds of different cross-linking degrees. Each sample follows the algorithm as shown in Fig 2. The hydrogel scaffolds were made from the same alginate and gelatin solution but introduced different concentrations of cross-linking agent.

DISCUSSION

The cumulative training time for a single sample using CNNs can vary up to several hours. While this may at times be longer than the time required to manually segment slices to interpolate using Biomedisa or Avizo, it's important to note the efficiency of SSSSeg in repeated samples. Interpolation-based methods demands manual work put into every dataset. Whereas in contrast, once the parameters for SSSSeg are known for a material, the same parameters can be used for datasets consisting of the same/similar material as the method is physics-driven. This:

1. **Streamlines the segmentation process for batch processing**
2. **Eliminates time devoted individual datasets**
3. **Does not require active monitoring**

The greatest potential of SSSSeg is that it is a strategy. No single step in the proposed method is limited to what was shown in Fig 2. Filtered back projection (FBP) was the primary CT reconstruction algorithm used, but there exist other algorithms each with their own merits. Gridrec is faster than FBP but requires more X-ray projections. Iterative reconstruction algorithms can work with fewer projections and are also suitable situations that call for low radiation dose. TIE-Hom is a pre-processing phase retrieval technique, it is applied to the raw data before CT reconstruction, but there are also post-processing phase retrieval and the GAN-based phase retrieval. As a strategy, SSSSeg can be used with a different phase retrieval algorithm just as it can work with a different CT reconstruction algorithm, image processing filters, CNN training architectures, and loss functions.

CONCLUSION

The effectiveness of SSSSeg on hydrogel scaffolds showed superior or comparative results to a prevailing method like Biomedisa. This allows efficient batch processing for segmentation of similar materials and significantly decreases the need for manual segmentation. As a semi-supervised technique, the only manual work is in determining the optimal CT reconstruction parameters. Although the method encountered challenges with lower contrast datasets, lower crosslinked hydrogels, the segmentation quality consistently remained within 5% of the leading segmentation tools. The results achieved show the potential for refining and expanding the application of SSSSeg in the analysis of similarly low-contrast materials.

REFERENCES

- [1] Mayo and Endrizzi, *Handbook of Advanced Nondestructive Evaluation*, 2019, [2] Losel et al., *Nat Commun*, 2020, [3] Henedriksen et al., *IEEE Trans Comput Imaging*, 2020, [4] Chen et al., *Bioactive Materials*, 2023, [5] Duan et al., *Comput Biol Med*, 2023, [6] Ning et al., *ACS Appl Mater Interfaces*, 2021, [7] Paganin et al., *J Microsc*, 2002

ACKNOWLEDGEMENTS

